*Proc. Natl. Acad. Sci. USA*
Vol. 88, pp. 9809–9812, November 1991
Biophysics

# Ultrafast spectroscopy of the visual pigment rhodopsin

(bathorhodopsin/subpicosecond/absorption/primary processes)

MING YAN†, D. MANOR‡, G. WENG‡, H. CHAO†, L. ROTHBERG§, T. M. JEDJU§, R. R. ALFANO†, AND R. H. CALLENDER‡¶

†Institute of Ultrafast Spectroscopy and Lasers and Departments of Physics and Electrical Engineering, City College of City University, New York, NY 10031; ‡Department of Physics, City College of City University, New York, NY 10031; and §AT&T Bell Laboratories, Murray Hill, NJ 07974

*Communicated by M. A. El-Sayed, August 5, 1991*

ABSTRACT **We report on time-resolved absorption studies of the bovine visual pigment rhodopsin with subpicosecond resolution at room temperature. Our data show that bathorhodopsin, rhodopsin's early photoproduct, is photochemically formed in 3.0 ± 0.7 ps. The data suggest that bathorhodopsin formation is kinetically preceded by two species along the rhodopsin-to-bathorhodopsin reaction coordinate. The first is identified with the vertically excited Franck–Condon state. This decays with an ≈200-fs lifetime to an intermediate, which then decays to bathorhodopsin in 3.0 ps. We assign this intermediate to be an excited state transient near 90° along the 11–12 torsional coordinate of rhodopsin's chromophore. Exchange of rhodopsin's exchangeable protons for deuterons does not affect the observed dynamics. These observations are both qualitatively and quantitatively consistent with molecular dynamics calculations, which model the rhodopsin to bathorhodopsin phototransition as a cis–trans isomerization along the 11–12 torsional coordinate of rhodopsin's chromophore.**

In vision, light is sensed when absorbed by special photoreceptor proteins, called rhodopsins, present in the rod and cone cells of eyes. These proteins contain a retinyl chromophore (a vitamin A derivative) bonded to the apoprotein by a protonated Schiff base linkage. There is a large body of evidence suggesting that the role of light is the photoexcitation of 11-*cis*-retinyl (structure **1**), the chromophore found in rhodopsin, to the trans form, forming a photoproduct called bathorhodopsin (cf. ref. 1). Bathorhodopsin is thermally unstable at room temperature, decaying on the nanosecond time scale to various thermal products leading to visual excitation. Light plays no further role in these processes.

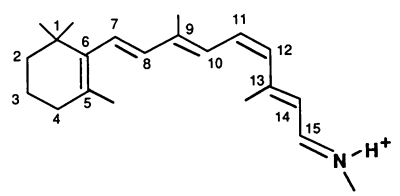


**1**

Several years ago, a number of experiments were attempted to determine the kinetic steps during the rhodopsin to bathorhodopsin transition (2–8). Rhodopsin ($\lambda_{max}$ = 498 nm for bovine rhodopsin) and bathorhodopsin ($\lambda_{max}$ = 543 nm) differ substantially in their absorption maxima and are, therefore, easily studied by transient absorption spectroscopy. The fastest of these studies, using instrumental time resolution of ≈6 ps, was not able to resolve the rhodopsin to bathorhodopsin photoconversion at room temperature, although an approximate time of ≈3 ps was estimated (4, 5). An intriguing result measured at low temperatures (<20 K), where the kinetics are slowed sufficiently to permit measurements with 6-ps resolution on rhodopsin suspended in a water/ethylene glycol glass, showed that bathorhodopsin formation is substantially retarded in rhodopsin where the exchangeable protons are deuterated. Moreover, the kinetics did not follow Arrhenius behavior (3, 9). The large isotope effect and non-Arrhenius behavior were taken as evidence for quantum mechanical tunneling of the proton along the protonated Schiff base hydrogen bond during the photoexcitation process leading to bathorhodopsin.

Recent improvements in ultrafast optical pulse generation have made sensitive measurements on subpicosecond time scales possible. Here, we undertake similar studies of the early photochemistry of rhodopsin in both protonated and deuterated aqueous environments at 295 K using subpicosecond pump and probe pulses. Thus, the resolution used here is more than a factor of 10 better than previous measurements. We observe that bathorhodopsin forms in 3.0 ± 0.7 ps in both $H_2O$ and $^2H_2O$ solvents. Moreover, the results suggest that at least two transient species precede bathorhodopsin formation.

## MATERIALS AND METHODS

**Sample Preparation.** Bovine rod outer segments were isolated from frozen retinas by the sucrose step gradient as described (5). Samples were washed with 10 mM Hepes (in either $H_2O$ or $^2H_2O$) and then solubilized in 20 mM *n*-dodecyl maltoside/0.1 M hydroxylamine/10 mM Hepes, adjusted to pH (or p$^2$H) 7.0. Under these conditions, the Schiff base proton (as well as other protein exchangeable protons) is known to be exchanged (10). The solubilized sample ($OD_{500}$ ≈ 2) was placed in an ice-chilled reservoir and circulated through a 1-cm-pathlength cuvette by a peristaltic pump. The flow rate was such that after each laser pulse the absorbing sample was completely replenished (11).

**Spectroscopy.** For generation of the primary pulses, two alternative laser systems were used. One is an amplified colliding pulse modelocked laser (20 Hz, 0.1 ps, 0.5 mJ), while the second utilizes a high repetition rate synchronously pumped dye laser (540 Hz, 0.3 ps, 0.5 mJ). In both cases, the primary pulses are used to generate "white" light continuum by focusing into a cell of flowing water. This white light is then split into two parts. One part, to be used as pump pulse, is passed through a 10-nm-bandpass filter centered at 500 nm and further amplified to ≈1 μJ per pulse in a cell of flowing coumarin 500 dye. The remainder of the white light (probe pulse) is filtered through various 10-nm-bandpass interference filters to probe at these wavelengths one at a time (≈10 nJ). The pump and probe are made collinear and focused to ≈500-μm spot size in the sample, and transmitted light is detected with a photomultiplier tube. An additional photo-

The publication costs of this article were defrayed in part by page charge payment. This article must therefore be hereby marked "*advertisement*" in accordance with 18 U.S.C. §1734 solely to indicate this fact.

¶To whom reprint requests should be addressed.

multiplier tube (reference) monitors the probe pulse intensity and is used to normalize all data for such fluctuations. A variable pathlength delay between pump and probe is used to map out the dynamics at each wavelength. Typically, 500 pump-induced transients are acquired together with 500 shots with the pump beam blocked. The two normalized sets are then divided by each other to obtain the actual transmission change, $\Delta T/T$. The two systems are essentially identical with regard to the pump pulse generation. While the high repetition rate laser is advantageous for low flux measurements (e.g., $\Delta T/T = 0.1\%$), the colliding pulse modelocked laser system has a better time resolution (300 fs vs. 1 ps). Kinetic profiles of data collected with either system were essentially identical.

**Data Analysis.** The kinetics of bathorhodopsin formation could not be fitted to a single exponential term. The simplest model involving the sequential formation of intermediates requires then that two transient species precede bathorhodopsin formation. As discussed below, we took these species to be the excited Franck–Condon state and a 90° isomerization intermediate. The populations of rhodopsin, $N_r(t)$, excited Franck–Condon state, $N_{fc}(t)$, excited 90° state, $N_{90}(t)$, and bathorhodopsin state, $N_b(t)$, are described in the following rate equations:

$$\frac{\partial N_r(t)}{\partial t} = (1-\eta)\frac{N_{90}(t)}{\tau_2} - \alpha I_p(t) N_r(t)$$

$$\frac{\partial N_{fc}(t)}{\partial t} = -\frac{N_{fc}(t)}{\tau_1} + \alpha I_p(t) N_r(t)$$

$$\frac{\partial N_{90}(t)}{\partial t} = \frac{N_{fc}(t)}{\tau_1} - \frac{N_{90}(t)}{\tau_2}$$

$$\frac{\partial N_b(t)}{\partial t} = \eta\frac{N_{90}(t)}{\tau_2},$$

where $I_p(t)$ is the pump pulse intensity, $\eta$ is the fraction of $N_{90}$ that converts to bathorhodopsin (assumed to be 0.67; the remainder is assumed to convert to rhodopsin according to the scheme given below), and $\alpha$ is defined as $\sigma/h\nu$ at the pump wavelength (500 nm). The total absorption change is described by

$$\Delta A(t) = \sigma_{90} N^*_{90}(t) + \sigma_{batho} N^*_b(t) + \sigma_{fc} N^*_{fc}(t) + \sigma_r(N^*_r(t) - N^*_r(-\infty)),$$

where $\sigma_{90}$, $\sigma_{fc}$, and $\sigma_{batho}$ are the absorption cross-sections of the 90°, Franck–Condon, and bathorhodopsin species, respectively. $N^*$ is the convolution of $N$ with the probe pulse $I_b(t)$. Solving the kinetic equations yields the absorption change, $\Delta A(t)$. It is a two-exponential decay convoluted with the pump probe laser cross-correlation function $P(t)$

$$\Delta A(t) = (a_1 e^{-t/\tau_1} + a_2 e^{-t/\tau_2} + a_3) \otimes P(t),$$

where

$$a_1 = \sigma^*_{fc} - \frac{\tau_2}{\tau_2 - \tau_1}\sigma^*_{90} + \frac{\eta\tau_1}{\tau_2 - \tau_1}\sigma^*_{batho}$$

$$a_2 = \frac{\tau_2}{\tau_2 - \tau_1}(\sigma^*_{90} - \eta\sigma^*_{batho})$$

$$a_3 = \eta\sigma^*_{batho},$$

and

$$\sigma^*_i = \sigma_i - \sigma_r.$$

The rate equations for the four states were solved analytically by using a gaussian representation of the pump and probe pulses, and the experimental data were numerically fitted to the resultant absorption term. The fitting result included two lifetimes and three amplitudes, which, in turn, can be solved for the absorption difference cross-sections of the intermediates involved.

## RESULTS AND DISCUSSION

Fig. 1*A* illustrates the transient change in absorption at 620 nm after excitation at 500 nm. The data clearly indicate a rapidly (unresolved) formed transient, which decays to a long-lived species. Measurements up to 100 ps showed no further significant changes in transmission. In particular, the changes previously reported (7, 8) were not observed, although these reported changes in transmission would be at just our signal/noise levels. In these previously reported experiments, the observed transient absorption spectrum maximum shifted slightly to the blue from early times to later times, and it was suggested that bathorhodopsin was formed by a precursor, called photorhodopsin, with a time constant of ≈40 ps (7). In what follows, we shall assume for discussion that the species we observe from 3 to 100 ps corresponds to

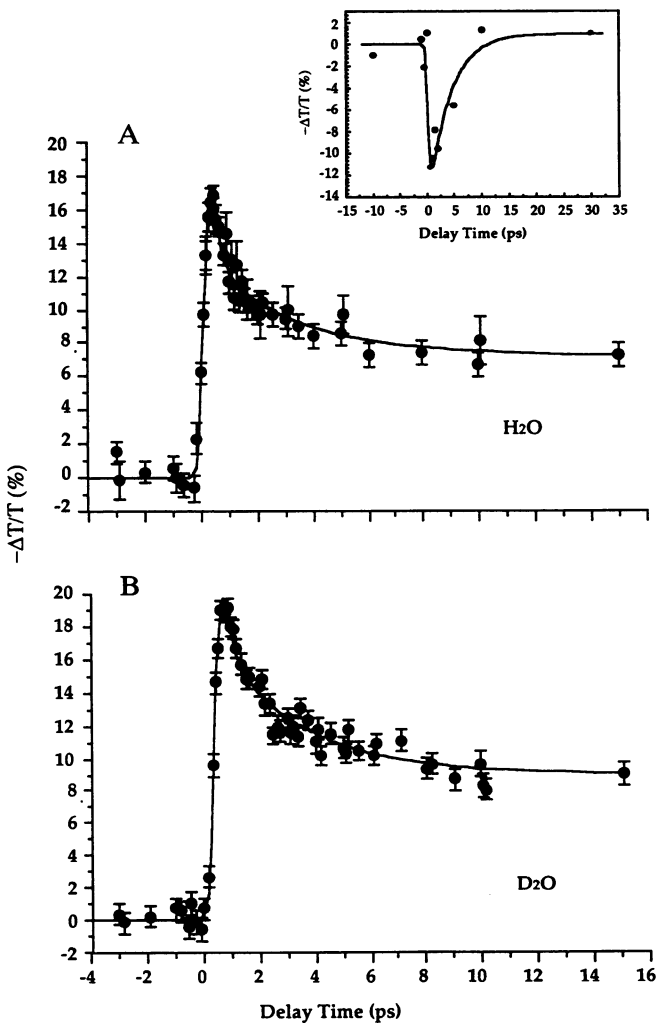


FIG. 1. (*A*) Absorption change at 620 nm induced by a 500-nm pump pulse as a function of pump probe delay time. The time resolution is ≈300 fs. The points are the data and the solid line is the calculated fit discussed in the text. (*Inset*) Analogous dynamics taken with a probe wavelength of 525 nm. (*B*) The same as in *A* except the samples were deuterated.

bathorhodopsin (see below). The induced decrease in transmission at long times is ≈0.5% for an excitation fluence $F$ of $1 \times 10^{15}$ photons per cm$^2$. This corresponds to a probability $\sigma F$ of 0.16 that a given molecule at the front of the sample cell is photoexcited where $\sigma$ is the known rhodopsin absorption cross-section at 500 nm. Direct measurements of incident power agree with this estimate. The maximum amplitude of the transient absorption is linear with pump fluence for incident power levels of up to $2 \times 10^{16}$ photons per cm$^2$. The shape of the dynamics shown in Fig. 1 is also nearly indistinguishable over this power range. In addition, the shape of the curve is indistinguishable, within our signal/noise, using probe wavelengths from 580 to 620 nm. The transmission decrease peaks near 580 nm, essentially the maximum of the bathorhodopsin–rhodopsin absorption difference spectrum (5). The inset to Fig. 1*A* shows the transmission kinetics recorded at 525 nm, very close to the isosbestic point between rhodopsin and bathorhodopsin. An unresolved increase in transmission is observed that recovers with a 3.0-ps time constant. Thus, absorption changes resulting from rhodopsin depletion are balanced by bathorhodopsin formation. Fig. 1*B* shows the same experiment as Fig. 1*A* except the sample is suspended in $^2H_2O$ buffer. No difference in the kinetic profile between Fig. 1 *A* and *B* is observed within our signal/noise. The same was true over the entire 550- to 620-nm wavelength range.

We were unable to fit our data to a single exponential term. This is evident from the data of Fig. 1; the shape of bathorhodopsin formation kinetics clearly cannot be represented by a single exponential. The data, however, are satisfactorily fitted by a sum of two exponential decays, implying that two transient species exist between rhodopsin and bathorhodopsin. A least-squares fit to the data yielded kinetic lifetimes of 200 ± 100 fs and 3.0 ± 0.7 ps for these two species using the data reduction procedures discussed in *Materials and Methods*. At 525 nm, near the isosbestic point between rhodopsin and bathorhodopsin, the contribution of the fast component is minimal. In this case, the transient kinetics are dominated by bathorhodopsin formation, which has a rise time of 3 ps (Fig. 1 *Inset*). Using the kinetic parameters from this fit and the assumed reaction scheme as defined in *Materials and Methods*, the spectra for the two transients can be calculated (relative to that of rhodopsin). The results from this calculation are plotted in Fig. 2. As the shape of the biexponential changes varies little over most of the measured wavelength range, the relative variation in the calculated spectra for the two intermediates is nearly the same from about 540 to 620 nm.

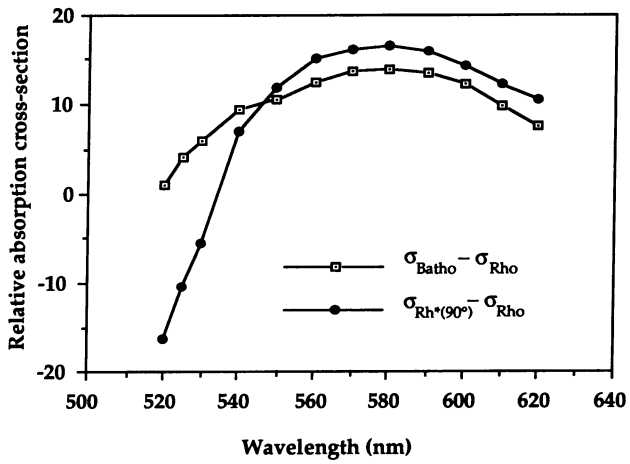


FIG. 2. The difference absorption cross-sections of bathorhodopsin and its kinetic precursor, identified as Rh*(90°), minus that of rhodopsin as calculated from the kinetic fits to the data. Error is ±10%. The *y* axis units are arbitrary. Note that while the difference between the two cross-sections is small over most of the wavelength range, the effect of the two species on the transient absorption spectra in this range differs substantially. The two species, Rh*(90°) and bathorhodopsin, contribute differently to the observed absorption kinetic profiles in our analysis through the parameter $\eta$, taken to be 0.67. For a different value of $\eta$, the relative ratio of the two cross-sections would scale accordingly.

It is widely agreed that the major change in the rhodopsin to bathorhodopsin transformation involves an 11-*cis* to 11-*trans* torsional rotation of the retinal chromophore [cf. ref. 1 for a recent review; a recent study suggests that the changes that take place in this photoreaction are mostly localized to the chromophore, while slower-formed subsequent thermal products involve substantial changes in the apoprotein (12)]. The potential surfaces along the 11-*cis* (rhodopsin) to 11-*trans* (bathorhodopsin) reaction coordinate have been quite well characterized and are depicted schematically in Fig. 3 (1, 14–18). Using this picture as a model for the observed kinetic events, the formation of bathorhodopsin starts by exciting rhodopsin to the vertically excited Franck–Condon species, Rh*(FC). Measurements of the fluorescence quantum yield from this species and theoretical calculations suggest that rotation out of the Franck–Condon region is on the order of 100 fs (18), in very good agreement with the observed 200-fs lifetime of the first transient species. It seems most likely that the Franck–Condon state decays to an excited state transient near 90°, which we will call Rh*(90°). Relaxation directly from the Franck–Condon state to an excited ground state is calculated to be very improbable (19). Thus, a scheme requiring two precursors that is consistent with this picture is given in Scheme I.

$$\text{Rh}(11\text{-}cis) \xrightarrow{h\nu} \text{Rh}^*(\text{FC}) \xrightarrow{\tau = 200\ \text{fs}} \text{Rh}^*(90°) \xrightarrow{\tau = 3\ \text{ps}} \text{batho}(trans)$$

Scheme I

According to the data of Fig. 2, the Rh*(90°) species has an absorption band profile similar to bathorhodopsin, perhaps slightly red shifted. There have been previous reports of a red-shifted precursor to bathorhodopsin (5).

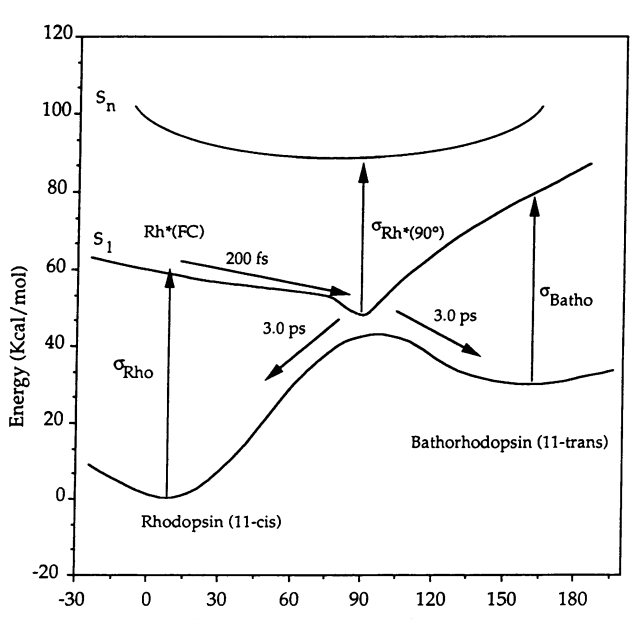


FIG. 3. Schematic potential surface for the cis–trans isomerization. Relevant times are described more precisely in the text. The general shapes of the curves are taken from ref. 13. The path in the excited state is taken simply from a single Franck–Condon state to the 90° position; this is obviously a simplification.

The kinetics measured here agree very well with molecular dynamic simulations of the primary photochemical event in rhodopsin by Birge and coworkers (13, 19, 20). In these calculations the 90° state is formed in ≈375 fs and bathorhodopsin is formed in ≈1.4 ps. Calculations of the early time-absorption spectra, from the formation of the Franck–Condon state to and including the 90° state, show several significant absorption bands in the visible range (R. Birge, personal communication). The weighted average of the calculated absorption spectrum during this time contains a band quite similar to bathorhodopsin. Our observation of an absorption difference band for Rh*(90°) centered near 580 nm (Fig. 2) is in good agreement with this.

Recent kinetic experiments on bacteriorhodopsin, a protein containing all-*trans* retinal, which is photoisomerized to 13-*cis* to a bathorhodopsin-like species, K, have been performed with femtosecond time resolution. The sequence of events determined in these measurements is similar to those we propose here (21–23). A state analogous to Rh*(90°), called $I_{460}$ or $bR^*(\tau_{13})$, is formed in ≈100 fs and decays to a state J, generally believed to be a ground state precursor to K, in ≈300 fs, which finally decays to K in ≈5 ps. However, our data on rhodopsin do not require two transient species between Rh*(FC) and bathorhodopsin. This difference requires further exploration with higher resolution.

Deuteration of rhodopsin has little, or no, effect on the dynamics according to the data of Fig. 1*B*. We conclude that there is no deuteration effect on the isomerization dynamics at 295 K. This is consistent with our expectation that the simple chromophore isomerization reaction scheme described in Fig. 2 will be unaffected by deuteration since the only chromophore proton that is deuterated is that bonded to the protonated Schiff base. We have no ready explanation for the large deuteration effect on the formation of bathorhodopsin that was previously observed at very low temperatures (3). It may be that the reaction coordinate at room temperature differs from that at low temperature because of constraints imposed on the protein when confined in a low-temperature glass, although this seems unlikely to us. A plausible explanation of the non-Arrhenius behavior and deuteration behavior has been proposed by Midler and Kliger (24). Using a theoretical approach of Englman and Jortner (25), which treats nonradioactive decay kinetics from a quantum mechanical point of view, curved Arrhenius plots might arise at very low temperatures, but not at room temperature, because of coupling between the chromophore isomerization and low frequency (≈50 $cm^{-1}$) modes of the apoprotein. In this view, the observed deuteration effect results from a change in the characteristic frequency of the apoprotein's low-frequency mode rather than proton tunneling, and the effect could very well not be observed at room temperature even though chromophore isomerization is occurring at both temperatures. In any case, proton tunneling or translocation, as deduced by Peters *et al.* (3) in their kinetic measurements of bathorhodopsin formation near liquid helium temperatures, appears to be unimportant in describing how rhodopsin is photochemically transformed to bathorhodopsin at physiological temperatures.

The authors wish to thank A. A. Gorokhovskii for his expert help in the laser setup and Robert Birge for helpful discussions. This work is supported in part by grants from the National Institutes of Health (EYO3142 to R.H.C. and RR-03060 to City College), by organized research funds to the Institute for Ultrafast Spectroscopy and Lasers, and by Hamamatsu Photonics and Mediscience Technology to R.R.A.

1. Birge, R. R. (1990) *Biochim. Biophys. Acta* **1016**, 293–327.
2. Bush, G. E., Applebury, M. L., Lamola, A. A. & Rentzepis, P. M. (1972) *Proc. Natl. Acad. Sci. USA* **69**, 2802–2806.
3. Peters, K., Applebury, M. L. & Rentzepis, P. M. (1977) *Proc. Natl. Acad. Sci. USA* **74**, 3119–3123.
4. Green, B. H., Monger, T. G., Alfano, R. R., Aton, B. & Callender, R. H. (1977) *Nature (London)* **269**, 179–180.
5. Monger, T. G., Alfano, R. R. & Callender, R. H. (1979) *Biophys. J.* **27**, 105–116.
6. Doukas, A. G., Stefancic, V., Suzuki, T., Callender, R. H. & Alfano, R. R. (1980) *Photobiochem. Photobiophys.* **1**, 305–308.
7. Shichida, Y., Matuoka, S. & Yoshizawa, T. (1984) *Photobiochem. Photobiophys.* **7**, 221–228.
8. Kandori, H., Matuoka, S., Shichida, Y. & Yoshizawa, T. (1989) *Photochem. Photobiol.* **49**, 181–184.
9. Applebury, M. L. (1984) *Vis. Res.* **24**, 1445–1454.
10. Oseroff, A. R. & Callender, R. (1974) *Biochemistry* **13**, 4243–4248.
11. Callender, R. H., Doukas, A., Crouch, R. & Nakanishi, K. (1976) *Biochemistry* **15**, 1621–1629.
12. Randall, C. E., Lewis, J. W., Hug, S. J., Bjorling, S. C., Eisner-Shanas, I., Friedman, N., Ottolenghi, M., Sheves, M. & Kliger, D. S. (1991) *J. Am. Chem. Soc.* **113**, 3473–3485.
13. Birge, R. (1990) *Annu. Rev. Phys. Chem.* **41**, 683–733.
14. Cooper, A. (1979) *Nature (London)* **282**, 531–533.
15. Honig, B., Ebrey, T., Callender, R., Dinur, U. & Ottolenghi, M. (1979) *Proc. Natl. Acad. Sci. USA* **76**, 2503–2508.
16. Schick, G. A., Cooper, T. M., Holloway, R. A., Murray, L. P. & Birge, R. R. (1987) *Biochemistry* **26**, 2556–2562.
17. Birge, R. R., Einterz, C. M., Knapp, H. M. & Murray, L. P. (1988) *Biophys. J.* **53**, 367–385.
18. Doukas, A. G., Junnarkar, M. R., Alfano, R. R., Callender, R. H., Kakitani, T. & Honig, B. (1984) *Proc. Natl. Acad. Sci. USA* **81**, 4790–4794.
19. Birge, R. R. & Hubbard, L. M. (1980) *J. Am. Chem. Soc.* **102**, 2195–2205.
20. Birge, R. R. & Hubbard, L. M. (1981) *Biophys. J.* **34**, 517–534.
21. Nuss, M. C., Zinth, W., Kaiser, W., Kolling, E. & Oesterhelt, D. (1985) *Chem. Phys. Lett.* **117**, 1–7.
22. Petrich, J. W., Breton, J., Martin, J. L. & Antonetti, A. (1987) *Chem. Phys. Lett.* **137**, 369–375.
23. Pollard, W. T., Cruz, C. H. B., Shank, C. V. & Mathies, R. A. (1989) *J. Chem. Phys.* **90**, 199–208.
24. Midler, S. J. & Kliger, D. S. (1986) *Biophys. J.* **49**, 567–570.
25. Englman, R. & Jortner, J. (1970) *Mol. Phys.* **18**, 145–164.